

Roles of positively charged dust, ion fluid temperature, and nonthermal electrons in the formation of modified-ion-acoustic solitary and shock waves

R. K. Shikha*, M. M. Orani, and A. A. Mamun
*Department of Physics & Wazed Mia Science Research Centre,
 Jahangirnagar University, Savar, Dhaka-1342, Bangladesh*

The dusty plasma system (containing nonthermally distributed inertialess electron species, warm inertial ion species, and positively charged stationary dust species) is considered. The basic features of subsonic and supersonic modified-ion-acoustic solitary and shock waves formed in such a dusty plasma system have been investigated by the reductive perturbation method. It has been shown that positively charged dust species plays a new role in favor of the formation of subsonic solitary and shock waves. On the other hand, the ion fluid temperature (represented by the parameter σ) and the electron nonthermal parameter (represented by α) play new significant roles in against the formation of subsonic solitary and shock waves, and give rise to the formation of the supersonic solitary and shock waves after their (σ 's and α 's) certain values. It is also shown that after a certain value of the nonthermal parameter α , the subsonic as well as supersonic solitary and shock waves are formed with negative potential. The important applications of the results of this theoretical investigation in space and laboratory dusty plasma systems are pinpointed.

PACS numbers: 52.27.Lw; 52.35.Sb; 52.35.Tc

I. INTRODUCTION

There has been a great deal of renewed interest in understanding the role of positively charged dust (PCD) species in modifying the existing features as well as in introducing new features of linear and nonlinear propagation of the modified-ion-acoustic (MIA) waves propagating in space [1–10] and laboratory [11–13] dusty plasma systems, where the PCD species coexists with the electron-ion plasmas. The dust species in such systems are positively charged [14] due to (i) secondary emission of electrons from the dust grain surface by the impact of high energetic plasma particles like electrons or ions [15], (ii) thermionic emission of electrons from the dust grain surface by the intense radiative or thermal heating [16], (ii) photo-emission of electrons from the dust grain surface by the interaction of high energy photons with the dust grain surface [17], etc.

The dispersion relation for the MIA waves in an electron-ion-PCD plasma system (containing inertialess Maxwellian electron species, inertial cold ion species, and stationary PCD species) is [18, 19]

$$\frac{\omega}{kC_i} = \frac{1}{\sqrt{1 + \mu + k^2\lambda_D^2}}, \quad (1)$$

where $\omega(k)$ is the MIA wave angular frequency (propagation constant); $C_i = (z_i k_B T_e / m_i)^{1/2}$ is the MIA speed in which k_B is the Boltzmann constant, T_e is the electron temperature, and m_i is the ion mass; $\lambda_D = (k_B T_e / 4\pi z_i n_{i0} e^2)^{1/2}$ is the MIA wave-length scale in which n_{i0} (z_i) is the number density (charge state) of the ion species at equilibrium, and e is the magnitude of

an electronic charge; $\mu = z_d n_{d0} / z_i n_{i0}$ with n_{d0} (z_d) being the number density (charge state) of the PCD species at equilibrium for which $n_{e0} = z_d n_{d0} + z_i n_{i0}$. This means that $\mu = 0$ corresponds to the electron-ion plasma, and $\mu \rightarrow \infty$ corresponds to electron-dust plasma [7, 11–13]. Thus, $0 < \mu < \infty$ is valid for the electron-ion-PCD plasmas. The dispersion relation (1) for the long-wavelength limit ($k\lambda_D \ll 1$) becomes

$$\frac{\omega}{kC_i} \simeq \sqrt{\frac{1}{1 + \mu}}. \quad (2)$$

The dispersion relation (2) indicates that the phase speed of the MIA waves decreases with the rise of the value of μ due to the reduction of the space charge electric field by the presence of the PCD species.

Recently, due to this new linear feature of the MIA waves, the subsonic solitary and shock waves exist in a dusty plasma system containing Maxwellian electron, cold ion, and PCD species [18, 19]. However, as indicated by (2) the reduction of the MIA wave phase speed due to the presence of the PCD species can also make the MIA phase speed comparable with the ion thermal speed $V_{Ti} = (k_B T_i / m_i)^{1/2}$ (where T_i is the ion fluid temperature) so that the effect of the ion-thermal pressure cannot be neglected. On the other hand, the electron species in many space environments does not always follow the Maxwellian velocity distribution function. This means that the dispersion relation (2), and the works [18, 19] are valid only for two limiting cases: (i) cold ion ($T_i = 0$) and (ii) Maxwellian electron species.

To overcome these two limitations, we consider (i) warm ion fluid ($T_i \neq 0$) [20] and (ii) nonthermal electron species following the Cairns velocity distribution function in the form [5]

$$f(v) = \frac{1 + \alpha(v^2 - 2\phi)^2}{(1 + 3\alpha)\sqrt{2\pi}} \exp\left[-\frac{1}{2}(v^2 - 2\phi)\right], \quad (3)$$

*Corresponding author: shikha152phy@gmail.com

where ϕ is the MIA wave potential normalized by $k_B T_e / e$, α is a parameter determining the population of the fast (energetic) particles present in the plasma system under consideration. We note that the distribution function defined by (3) is identical to the Maxwellian electron distribution function for $\alpha = 0$. How this nonthermal parameter α modifies the Maxwell distribution curve of the electron species is shown in figure 1. The effects of the

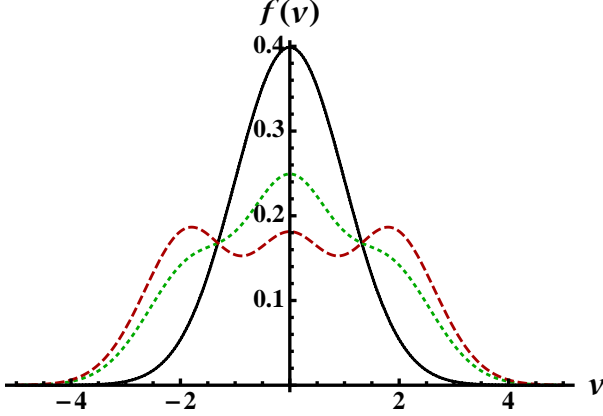


FIG. 1: How the different values of α [viz. $\alpha = 0$ (solid curve), $\alpha = 0.2$ (dotted curve), and $\alpha = 0.4$ (dashed curve)] deviate from the curve corresponding to the Maxwellian distribution function to that corresponding to the Cairns distribution function [5]. We note that $\phi = 0.5$ is used.

Cairns nonthermal electron distribution (α) and the ion fluid temperature ($\sigma = T_i / z_i T_e$) reduces the dispersion relation (2) for the long wavelength MIA waves to

$$\frac{\omega}{kC_i} = \sqrt{\sigma + \frac{1 + 3\alpha}{(1 + \mu)(1 - \alpha)}}. \quad (4)$$

The dispersion relation (4) indicates that as α and σ increase, the phase speed of the MIA waves increases and decreases the ion Landau damping [21]. This is due to the enhancement of the space charge electric field by the nonthermal electron species and by the thermal temperature of ion species. The aim of this work is to investigate the combined effects of the PCD species, Cairns nonthermal electron species, and ion fluid temperature on the basic features of the MIA solitary (shock) waves in the electron-ion-PCD plasma system by deriving the Korwege-de Vries (KDV) equation [22, 23] (Burgers equation [23–25]).

The manuscript is structured in the following manner. The governing equations are provided in section II. The basic features of solitary (shock) waves, are investigated by making use of the reductive perturbation method [22–25] in section III (IV). A brief discussion on our theoretical work is presented in section V.

II. GOVERNING EQUATIONS

We consider a plasma system containing nonthermally distributed inertialess electron species [following the Cairns distribution function represented by (3)], isothermal warm inertial ion species, and stationary PCD species. The nonlinear dynamics of the MIA waves in this electron-ion-PCD plasma system is governed by the normalized equations in the form

$$\frac{\partial n_i}{\partial t} + \frac{\partial}{\partial x}(n_i u_i) = 0, \quad (5)$$

$$\frac{\partial u_i}{\partial t} + u_i \frac{\partial u_i}{\partial x} = -\frac{\partial \phi}{\partial x} - \frac{\sigma}{n_i} \frac{\partial n_i}{\partial x} + \eta \frac{\partial^2 u_i}{\partial x^2}, \quad (6)$$

$$\frac{\partial^2 \phi}{\partial x^2} = (1 + \mu)n_e - n_i - \mu, \quad (7)$$

where n_i (n_e) is the ion (electron) number density normalized by n_{i0} (n_{e0}); u_i is the ion fluid speed normalized by C_i ; $x(t)$ is the space (time) co-ordinate normalized by λ_D (ω_{pi}^{-1}); η is the ion fluid kinematic viscosity coefficient [19] normalized by $\omega_{pi} \lambda_D^2$.

The expression for n_e is obtained by integrating the non-thermal Cairns distribution function [defined by (3)] over the whole velocity space, i.e.

$$n_e = \int_{-\infty}^{\infty} f(v) dv = (1 - \beta\phi + \beta\phi^2) \exp(\phi), \quad (8)$$

where $\beta = 4\alpha / (1 + 3\alpha)$. It indicates for $\alpha = 0$ that $n_e = \exp(\phi)$ yielding the Maxwellian electron species.

III. KDV SOLITARY WAVES

To study the nature of the KDV solitary waves in the electron-ion-PCD plasma system under consideration, we first stretch the independent variables x and t as [22, 23]

$$\zeta = \epsilon^{\frac{1}{2}}(x - \mathcal{V}_p t), \quad (9)$$

$$\tau = \epsilon^{\frac{3}{2}} t, \quad (10)$$

where ϵ is the small dimensionless expansion parameter, \mathcal{V}_p is the MIA wave phase speed normalized by C_i indicating $\mathcal{V}_p = \omega / kC_i$, and ζ (τ) is normalized as x (t) is. We then expand the dependent variables n_i , u_i , and ϕ as [22, 23]

$$n_i = 1 + \epsilon n_i^{(1)} + \epsilon^2 n_i^{(2)} + \dots, \quad (11)$$

$$u_i = 0 + \epsilon u_i^{(1)} + \epsilon^2 u_i^{(2)} + \dots, \quad (12)$$

$$\phi = 0 + \epsilon \phi^{(1)} + \epsilon^2 \phi^{(2)} + \dots. \quad (13)$$

We now develop the equations in various powers of ϵ . To the lowest-order approximation, we obtain

$$n_i^{(1)} = \frac{1}{\mathcal{V}_p^2 - \sigma} \phi^{(1)}, \quad (14)$$

$$u_i^{(1)} = \frac{\mathcal{V}_p}{\mathcal{V}_p^2 - \sigma} \phi^{(1)}, \quad (15)$$

$$\mathcal{V}_p = \sqrt{\sigma + \frac{1 + 3\alpha}{(1 + \mu)(1 - \alpha)}}. \quad (16)$$

This is the linear dispersion for the MIA waves in the electron-ion-PCD plasma system, and is identical to (4) since $\mathcal{V}_p = \omega/kC_i$. The interpretation of (4) is verified graphically by displaying the figures 2 and 3 which show how \mathcal{V}_p varies with μ , α , and σ .

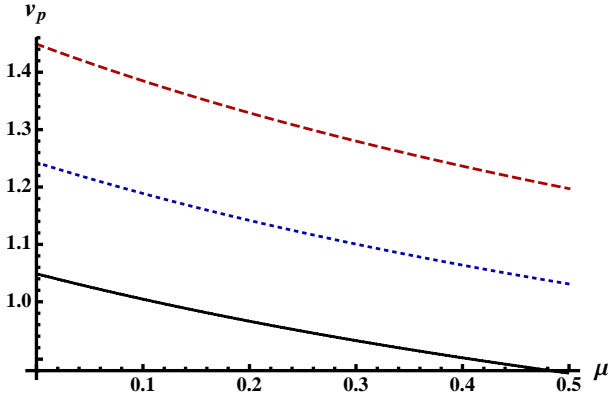


FIG. 2: The variation of \mathcal{V}_p with μ for different values of α [viz. $\alpha = 0$ (solid curve), $\alpha = 0.1$ (dotted curve), and $\alpha = 0.2$ (dashed curve)] and $\sigma = 0.1$.

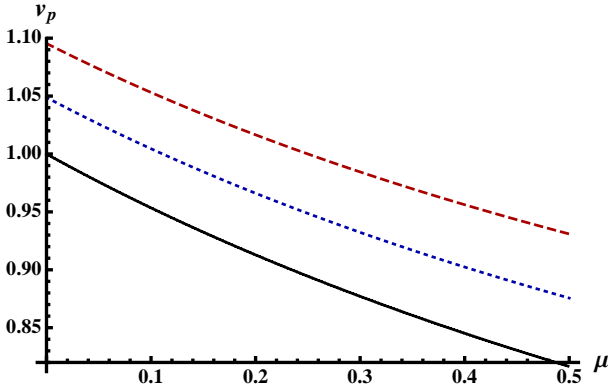


FIG. 3: The variation of \mathcal{V}_p with μ for different values of σ [viz. $\sigma = 0$ (solid curve), $\sigma = 0.1$ (dotted curve), and $\sigma = 0.2$ (dashed curve)] and $\alpha = 0$.

To the next higher order approximation, we obtain

$$\frac{\partial n_i^{(1)}}{\partial \tau} - \mathcal{V}_p \frac{\partial n_i^{(2)}}{\partial \zeta} + \frac{\partial u_i^{(2)}}{\partial \zeta} + \frac{\partial}{\partial \zeta} [n_i^{(1)} u_i^{(1)}] = 0, \quad (17)$$

$$\frac{\partial u_i^{(1)}}{\partial \tau} - \mathcal{V}_p \frac{\partial u_i^{(2)}}{\partial \zeta} + \gamma u_i^{(1)} \frac{\partial u_i^{(1)}}{\partial \zeta} = -\frac{\partial \phi^{(2)}}{\partial \zeta} - \sigma \frac{\partial n_i^{(2)}}{\partial \zeta}, \quad (18)$$

$$\frac{\partial^2 \phi^{(1)}}{\partial \zeta^2} = (1 + \mu)(1 - \beta) \phi^{(2)} + \frac{1}{2}(1 + \mu) [\phi^{(1)}]^2 - n_i^{(2)}, \quad (19)$$

where $\gamma = 1 + \sigma/\mathcal{V}_p^2$, which is obtained from (14) and (15). We finally use (14)–(19) to obtain the KDV equation in the form

$$\frac{\partial \phi^{(1)}}{\partial \tau} + \mathcal{A} \phi^{(1)} \frac{\partial \phi^{(1)}}{\partial \zeta} + \mathcal{B} \frac{\partial^3 \phi^{(1)}}{\partial \zeta^3} = 0, \quad (20)$$

where \mathcal{A} and \mathcal{B} denote the nonlinear and dispersion coefficients, which are, respectively, given by

$$\mathcal{A} = \left[\frac{(3\mathcal{V}_p^2 + \sigma) - (1 + \mu)(\mathcal{V}_p^2 - \sigma)^3}{2\mathcal{V}_p(\mathcal{V}_p^2 - \sigma)} \right], \quad (21)$$

$$\mathcal{B} = \frac{(\mathcal{V}_p^2 - \sigma)^2}{2\mathcal{V}_p}. \quad (22)$$

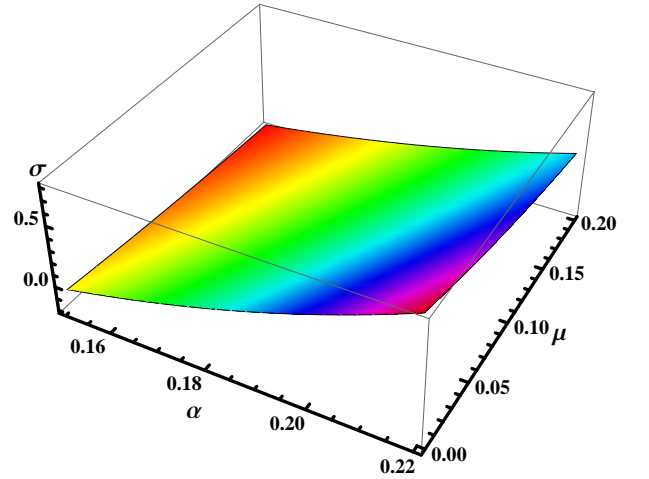


FIG. 4: $\mathcal{A} = 0$ surface plot showing the parametric regimes for the existence of the KDV solitary waves with $\phi > 0$ (parametric space $\{\mu, \alpha, \sigma\}$ above $\mathcal{A} = 0$ surface) and $\phi < 0$ (parametric space $\{\mu, \alpha, \sigma\}$ below $\mathcal{A} = 0$ surface).

The stationary solitary wave solution of the KDV equation (20) is derived by considering a moving frame $\xi = \zeta - \mathcal{U}_0 \tau$ (moving with a constant speed \mathcal{U}_0), where ξ is normalized as ζ is, and \mathcal{U}_0 is normalized by C_i . Now, imposing the appropriate boundary conditions, viz. $\phi^{(1)} \rightarrow 0$, $d\phi^{(1)}/d\zeta \rightarrow 0$, and $d^2\phi^{(1)}/d\zeta^2 \rightarrow 0$ at $\xi \rightarrow \pm\infty$. These assumptions lead to the stationary solitary wave solution of the KDV equation (20) in the form

$$\phi^{(1)} = \phi_m^{(1)} \text{sech}^2 \left(\frac{\xi}{\Delta} \right). \quad (23)$$

where $\phi^{(1)}$ (Δ) is the amplitude (width) of the MIA solitary waves, and are written as

$$\phi_m^{(1)} = \frac{3\mathcal{U}_0}{\mathcal{A}} \quad \text{and} \quad \Delta = \sqrt{\frac{4\mathcal{B}}{\mathcal{U}_0}}, \quad (24)$$

respectively. It is clear from (23)–(24) that the subsonic and supersonic solitary waves (of amplitude $3\mathcal{U}_0/\mathcal{A}$ and width $\sqrt{4\mathcal{B}/\mathcal{U}_0}$) exist with $\phi^{(1)} > 0$ [$\phi^{(1)} < 0$] for $\mathcal{A} > 0$ [$\mathcal{A} < 0$] since $\mathcal{U}_0 > 0$ and $\mathcal{B} > 0$ are always valid, and that amplitude (width) of the MIA solitary waves increases (decreases) directly with \mathcal{U}_0 ($\sqrt{\mathcal{U}_0}$). The parametric regimes corresponding to $\mathcal{A} > 0$ and $\mathcal{A} < 0$ are shown by displaying the $\mathcal{A} = 0$ surface plot in figure 4. To observe how the basic features (polarity, amplitude, and width) of the MIA solitary waves are modified by the number density of the stationary PCD species (represented by μ), the ion fluid temperature (represented by σ), and the nonthermal parameter α (representing the population of the fast or energetic electrons), we have graphically represented (23) for the different values of μ , σ , and α . The results are displayed in figures 5–8.

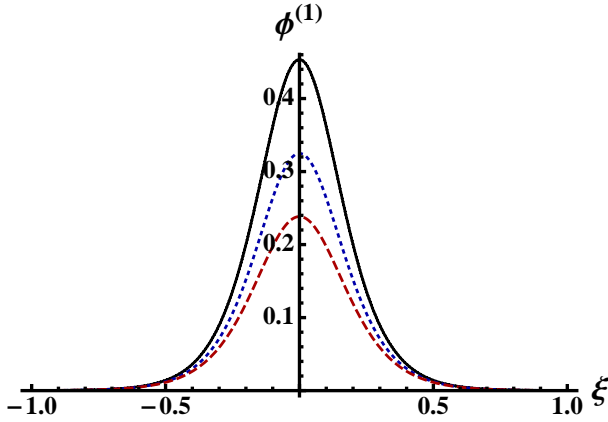


FIG. 5: The solitary potential profiles for $\mathcal{U}_0 = 0.1$, $\sigma = 0.1$, $\alpha = 0.1$, $\mu = 0.2$ (solid curve), $\mu = 0.3$ (dotted curve), and $\mu = 0.4$ (dashed curve).

IV. BURGERS SHOCK WAVES

To study Burgers shock waves in the dissipative electron-ion-PCD plasma system under consideration, we first stretch the independent variables x and t as [23–25]

$$\zeta = \epsilon(x - \mathcal{V}_p t), \quad (25)$$

$$\tau = \epsilon^2 t. \quad (26)$$

We then expand the dependent variables n_i , u_i , and ϕ by (11), (12), and (13), respectively. We again develop the equations in various powers of ϵ . To the lowest-order approximation, we obtain a linear set of equations, which are given by (14)–(16).

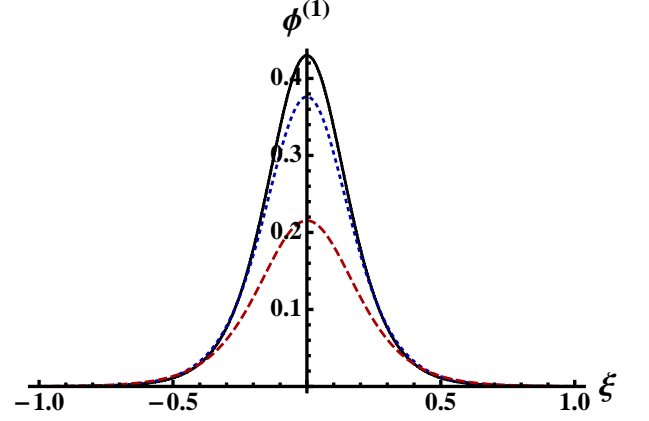


FIG. 6: The solitary potential profiles for $\mathcal{U}_0 = 0.1$, $\mu = 0.3$, $\alpha = 0.1$, $\sigma = 0$ (solid curve), $\sigma = 0.2$ (dotted curve), and $\sigma = 0.4$ (dashed curve).

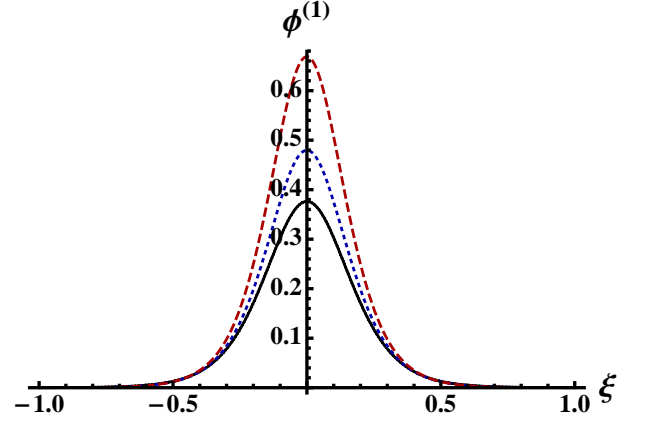


FIG. 7: The solitary potential profiles for $\mathcal{U}_0 = 0.1$, $\mu = 0.3$, $\sigma = 0.1$, $\alpha = 0.1$ (solid curve), $\alpha = 0.125$ (dotted curve), and $\alpha = 0.15$ (dashed curve).

To the next higher order approximation, we obtain

$$\frac{\partial n_i^{(1)}}{\partial \tau} - \mathcal{V}_p \frac{\partial n_i^{(2)}}{\partial \zeta} + \frac{\partial u_i^{(2)}}{\partial \zeta} + \frac{\partial}{\partial \zeta} [n_i^{(1)} u_i^{(1)}] = 0, \quad (27)$$

$$\begin{aligned} \frac{\partial u_i^{(1)}}{\partial \tau} - \mathcal{V}_p \frac{\partial u_i^{(2)}}{\partial \zeta} + u_i^{(1)} \frac{\partial u_i^{(1)}}{\partial \zeta} = & -\frac{\partial \phi^{(2)}}{\partial \zeta} - \sigma \frac{\partial n_i^{(2)}}{\partial \zeta} \\ & - \sigma n_i^{(1)} \frac{\partial n_i^{(1)}}{\partial \zeta} + \eta \frac{\partial^2 u_i^{(1)}}{\partial \zeta^2}, \end{aligned} \quad (28)$$

$$0 = (1 + \mu)(1 - \beta)\phi^{(2)} + \frac{1}{2}(1 + \mu) [\phi^{(1)}]^2 - n_i^{(2)}. \quad (29)$$

We finally use (14)–(16) and (27)–(29) to obtain the Burgers equation in the form

$$\frac{\partial \phi^{(1)}}{\partial \tau} + \mathcal{A} \phi^{(1)} \frac{\partial \phi^{(1)}}{\partial \zeta} = \mathcal{C} \frac{\partial^2 \phi^{(1)}}{\partial \zeta^2}, \quad (30)$$

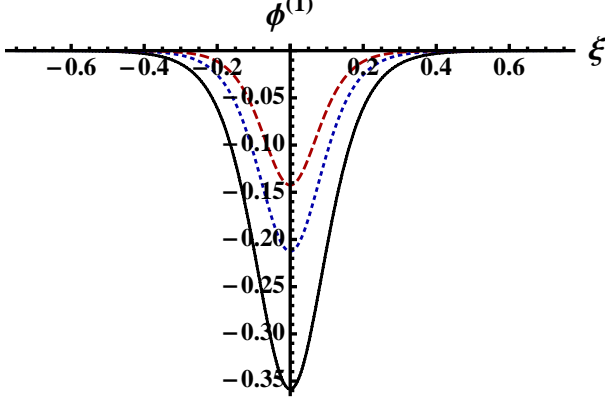


FIG. 8: The solitary potential profiles for $\mathcal{U}_0 = 0.1$, $\mu = 0.3$, $\sigma = 0.1$, $\alpha = 0.3$ (solid curve), $\alpha = 0.35$ (dotted curve), and $\alpha = 0.4$ (dashed curve).

where $\mathcal{A}(\mathcal{C})$ is the coefficient of nonlinearity (dissipation). The nonlinear coefficient \mathcal{A} is by (21), and the dissipative coefficient \mathcal{C} is given by $\mathcal{C} = \eta/2$. To obtain

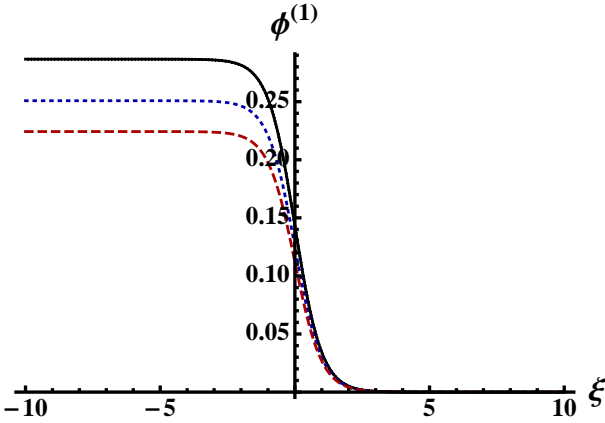


FIG. 9: The shock potential profiles for $\mathcal{U}_0 = 0.1$, $\sigma = 0.1$, $\alpha = 0.1$, $\eta = 0.1$, $\mu = 0.2$ (solid curve), $\mu = 0.3$ (dotted curve), and $\mu = 0.4$ (dashed curve).

the stationary shock wave solution of the Burgers equation (30), we again consider a moving frame moving with the speed \mathcal{U}_0 , i.e. $\xi = \zeta - \mathcal{U}_0\tau$, and impose the appropriate boundary conditions ($\phi^{(1)} \rightarrow 0$ and $d\phi^{(1)}/d\xi \rightarrow 0$ at $\xi \rightarrow \infty$). These assumptions lead to the stationary shock wave solution of the Burgers equation (30) in the form

$$\phi^{(1)} = \phi_m^{(1)} \left[1 - \tanh \left(\frac{\xi}{\Delta} \right) \right], \quad (31)$$

where $\phi_m^{(1)}$ is the amplitude and Δ is the width of the shock waves, are given by

$$\phi_m^{(1)} = \frac{\mathcal{U}_0}{\mathcal{A}}, \quad \text{and} \quad \Delta = \frac{\eta}{\mathcal{U}_0}. \quad (32)$$

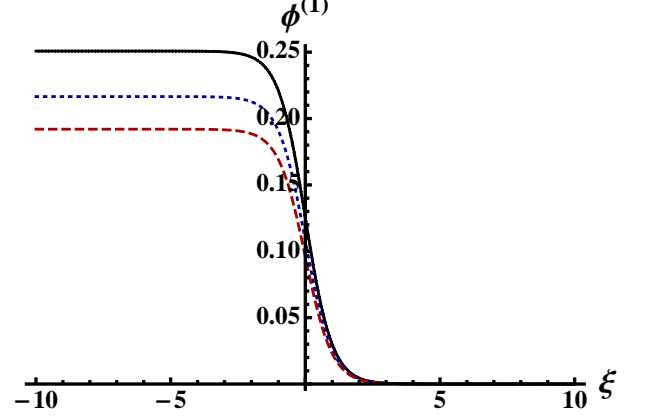


FIG. 10: The shock potential profiles for $\mathcal{U}_0 = 0.1$, $\mu = 0.3$, $\alpha = 0.1$, $\eta = 0.1$, $\sigma = 0.1$ (solid curve), $\sigma = 0.2$ (dotted curve), and $\sigma = 0.3$ (dashed curve).

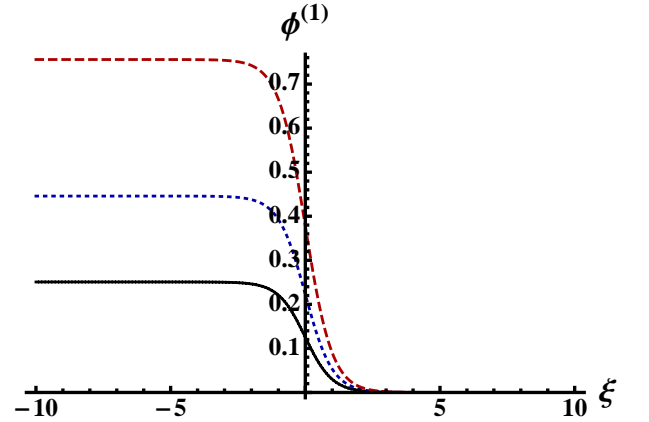


FIG. 11: The shock potential profiles for $\mathcal{U}_0 = 0.1$, $\mu = 0.3$, $\sigma = 0.1$, $\eta = 0.1$, $\alpha = 0.1$ (solid curve), $\alpha = 0.125$ (dotted curve), and $\alpha = 0.15$ (dashed curve).

It is obvious from (31) and (32) with figures 2-4 that the subsonic and supersonic shock waves are formed with $\phi > 0$ ($\phi < 0$) for $\mathcal{A} > 0$ ($\mathcal{A} < 0$). It is also clear that the width of the shock waves is directly (inversely) proportional to η (\mathcal{U}_0). However, to observe how the basic features (polarity, amplitude, and width) of the shock waves are modified by the number density of the stationary PCD species (represented by the parameter μ), the ion fluid temperature (represented by the parameter σ), and the nonthermal parameter α (representing the population of the fast or energetic electrons), we have graphically represented (31) for the different values of μ , σ , and α . The results are displayed in figures 9–12.

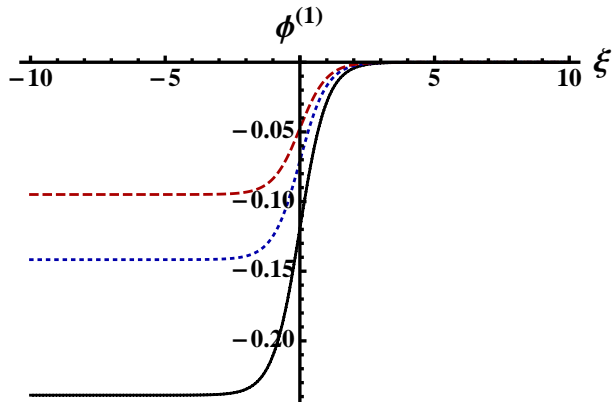


FIG. 12: The shock potential profiles for $U_0 = 0.1$, $\mu = 0.3$, $\sigma = 0.1$, $\eta = 0.1$, $\alpha = 0.3$ (solid curve), $\alpha = 0.35$ (dotted curve), and $\alpha = 0.4$ (dashed curve).

V. DISCUSSION

The dusty plasma system (containing inertialess non-thermal electron, warm inertial ion, and stationary PCD species) is considered. The roles of the stationary PCD species, ion fluid temperature, and nonthermal electrons in the linear and nonlinear propagation of the long (compared to λ_D) wavelength MIA waves in such a plasma system are identified. They can be pointed as follows:

- The phase speed of the long wavelength MIA waves decreases with the rise of the number density and charge of the stationary PCD species. This is due to the reduction of the space charge electric field (caused by the PCD species) in the electric field of the MIA waves in which inertia is provided by the positive ion fluid.
- The phase speed of the long wavelength MIA waves increases with the increase in the ion fluid temperature as well as in the fraction of the energetic electrons. This is due to the enhancement of the space charge electric field (caused by the more flexibility of the ion fluid and by the excess energy of the energetic/fast particles) in the electric field of the MIA waves in which restoring force comes from the electron species.
- The possibility for the formation of the subsonic solitary and shock waves increases with the rise of the number density and charge of the stationary PCD species, since the latter reduces the phase speed to its values of the subsonic range. But, this possibility decreases with the rise of the ion fluid temperature and with the rise of the fraction of the fast/energetic electrons since the latter enhance the phase speed to the supersonic range.
- The possibility for the formation of the subsonic solitary and shock waves with negative poten-

tial increases with the rise of the fraction of the fast/energetic electrons. But this possibility decreases with the rise of the number density and charge of the stationary PCD species as well as with the rise of the ion fluid temperature.

- The amplitude of the solitary and shock waves decreases with rise of the values of number density and charge of the PCD species and with the ion fluid temperature, but increases with the increase in the fraction of the fast/energetic electrons. The amplitude of the solitary waves is three times larger than that of the shock waves, but the nature of the variation of the shock and solitary wave amplitude are identical since the nonlinear coefficient in KDV and Burgers equations are identical.
- The width of the solitary waves increases with rise of the values of the number density and charge of the PCD species and with the ion fluid temperature, but decreases with the increase in the fraction of the fast/energetic electrons.

It is important to mention that to derive KDV equation, we use the stretched or rescaled co-ordinates [22], which is valid only when the effect of dissipation is negligible in comparison with that of the dispersion, and that to derive Burgers equation, we use the stretched or rescaled co-ordinates [24], which is valid only when the effect of dispersion is negligible in comparison with that of the dissipation. We have used the reductive perturbation method with these KDV [22] and Burgers [24] stretching to derive the KDV and Burgers equations, respectively.

The limitation of the reductive perturbation method is that it is not valid for the arbitrary amplitude solitary and shock waves. To overcome this limitation, one has to develop a numerical code to simulate the basic equations (5)–(7). This type of numerical simulation will be able to show the time evolution of arbitrary amplitude solitary and shock waves. This is, of course, a challenging research problem, but beyond the scope of our present work. However, the results of our present work should be useful in understanding the ion-acoustic disturbances in different space (viz. Earth's mesosphere [1–3], upper part of ionosphere [4, 5], cometary tails [6, 7], Jupiter's surroundings [8], Jupiter's magnetosphere [9], noctilucent clouds [10], etc.) and laboratory [11–13] dusty plasma systems, where the PCD species coexists with the electron-ion plasmas.

Barkan *et al.* [26] have performed a laboratory experiment on the propagation of the MIA waves in plasma system containing electron, ion, and negatively charged dust (NCD) species, and have shown that the presence of NCD species enhances the phase speed of the MIA waves. This experimental setup of Barkan *et al.* [26] is expected to verify our result that the presence of the PCD species reduces the phase speed of the MIA waves by using PCD species instead of NCD species. On the other hand, Nakamura *et al.* [27, 28] have performed two

laboratory experiments on the formation of solitary [27] and shock [28] waves in electron-ion-NCD plasmas. The basic features of the solitary and shock waves predicted

in our present investigation can be tested by the experimental setup of Nakamura *et al.* [27, 28] by replacing the NCD species by the PCD species.

-
- [1] O. Havnes, J. Trøim, T. Blix, W. Mortensen, L. I. Næsheim, E. Thrane, and T. Tønnesen, *J. Geophys. Res.* **101**, 10839 (1996).
 - [2] L. J. Gelinas, K. A. Lynch, M. C. Kelley, S. Collins, S. Baker, Q. Zhou, and J. S. Friedman, *Geophys. Res. Lett.* **25**, 4047 (1998).
 - [3] D. A. Mendis, Wai-Ho Wong, and M. Rosenberg, *Phys. Scripta* **T113**, 141 (2004).
 - [4] P. O. Dovner, A. I. Eriksson and Boström, *Geophys. Res. Lett.* **21**, 1827 (1994).
 - [5] R. A. Cairns, A. A. Mamun, R. Bingham, R. Boström, R. O. Dendy, C. M. C. Nairn, and P. K. Shukla, *Geophys. Res. Lett.* **22**, 2709 (1995).
 - [6] M. Horányi, *Annu. Rev. Astron. Astrophys.* **34**, 383 (1996).
 - [7] A. A. Mamun and P. K. Shukla, *Geophys. Res. Lett.* **31**, L06808 (2004).
 - [8] D. Tsintikidis, D. A. Gurnett, W. S. Kurth, and L. J. Granroth, *Geophys. Res. Lett.* **23**, 997 (1996).
 - [9] M. Horányi, G. E. Morfill, and E. Grün, *Nature London* **363**, 144 (1993).
 - [10] M. Rapp and F. J. Lübken, *Earth. Planet. Sp.* **51**, 799 (1999).
 - [11] S. A. Khrapak and G. Morfill, *Phys. Plasmas* **8**, 2629 (2001).
 - [12] V. E. Fortov, A. P. Nefedov, O. S. Vaulina, O. F. Petrov, I. E. Dranzhevski, A. M. Lipaev, and Y. P. Semenov, *New J. Physics* **5**, 102 (2003).
 - [13] A. E. Davletov, F. Kurbanov, and Y. S. Mukhametkarimov, *Phys. Plasmas* **25**, 120701 (2018).
 - [14] V. E. Fortov, A. P. Nefedov, O. S. Vaulina, A. M. Lipaev, V. I. Molotkov, A. A. Samaryan *et al.*, *J. Exp. Theor. Phys.* **87**, 1087 (1998).
 - [15] V. W. Chow, D. A. Mendis, and M. Rosenberg, *J. Geophys. Res.* **98**, 19065 (1993).
 - [16] M. Rosenberg and D. A. Mendis, *IEEE Trans. Plasma Sci.* **23**, 117 (1995).
 - [17] M. Rosenberg, D. A. Mendis, and D. P. Sheehan, *IEEE Trans. Plasma Sci.* **24**, 1422 (1996).
 - [18] A. A. Mamun, *Contrib. Plasma Phys.* **61**, e202000192 (2021).
 - [19] A. A. Mamun and B. E. Sharmin, *AIP Advances* **10**, 125317 (2020).
 - [20] A. A. Mamun, *Phys. Rev. E* **55** (2) (1997).
 - [21] A. A. Mamun and P. K. Shukla, *J. Plasma Phys.* **77**, 437 (2021).
 - [22] H. Washimi and T. Taniuti, *Phys. Rev. Lett.* **17**, 996 (1996).
 - [23] F. Deeba, S. Tasnim, and A. A. Mamun, *IEEE Trans. Plasma Sci.* **40**, 2247 (2012).
 - [24] A. A. Mamun and R. A. Cairns, *Phys. Rev. E* **79**, R055401 (2009).
 - [25] A. A. Mamun, *Phys. Plasmas* **26**, 084501 (2019).
 - [26] A. Barkan, N. D'Angelo, and R. L. Merlino, *Planet. Space Sci.* **44**, 239 (1996).
 - [27] Y. Nakamura and A. Sharma, *Phys. Plasmas* **8**, 3921 (2001).
 - [28] Y. Nakamura, H. Bailung, and P. K. Shukla, *Phys. Rev. Lett.* **83**, 1602 (1999).